YTUP

Journal of Thermal Engineering
https://jten.yildiz.edu.tr/
https://doi.org/10.47481/jten.0003

RESEARCH ARTICLE

Numerical investigation of an ammonia-hydrogen swirl burner

Mehmet Anil Gulsan[1,*], Yakup Erhan Boke[2]

[1]Department of Mechanical Engineering, Istanbul Technical University, Istanbul, 34437, Türkiye
[2]Department of Mechanical Engineering, Istanbul Technical University, Istanbul, 34437, Türkiye

Abstract

Combustion always plays a crucial role in scientific research due to its complexity and diversity. In recent years, the global trend towards decarbonization has accelerated interest in carbon-free combustion technologies. Additionally, increasing demand for energy has prompted researchers to seek alternative energy sources beyond hydrocarbons. Among these, ammonia has emerged as a promising carbon-free fuel due to its favorable thermo-chemical properties and well-established supply chain infrastructure. While extensive experimental research has been carried out on ammonia combustion, investigating all relevant parameters is still challenging due to the requirement for advanced measurement technologies. At the same time, developments in computational power have considerably improved the capabilities of numerical simulations. In this study, an industrial-scale tangential swirl burner was numerically simulated. A 50–50 ammonia-hydrogen fuel blend by volume was used under both rich (equivalence ratio of 1.2) and lean (equivalence ratio of 0.7) conditions at three different power levels (10, 15, and 20 kW). The study offers new insight by comparing different reaction mechanisms and evaluating their performance in predicting the combustion behavior of ammonia-hydrogen mixtures. The burner model was described in detail, and the simulations were carried out using three different reaction mechanisms. Experimental temperature and exhaust emission data were used for validation of the model. The results indicate that numerical models are able to predict temperature distributions with a maximum deviation of 9%, showing that numerical simulations are effective tools for analyzing ammonia-hydrogen combustion. These results emphasize the importance of validating numerical models against experimental data. The study also shows that advanced simulation approaches can contribute to optimizing ammonia-hydrogen burners while reducing the need for extensive experimental work. This may accelerate the development of ammonia-based combustion technologies. Although the results are promising, discrepancies in the prediction of NH_3 and NO_x suggest that the reaction mechanisms still require further refinement. In future work, artificial intelligence and advanced computational techniques could improve the accuracy of these models and support the transition toward zero-carbon energy systems.

Keywords: Burner, ammonia, hydrogen, cfd, combustion, emissions

Cite this article as: Gulsan, M. A., & Boke, Y. E. (2026). Numerical investigation of an ammonia-hydrogen swirl burner. Journal of Thermal Engineering, 12(3), 870–886. https://doi.org/10.47481/jten.0003

1. Introduction

As a carbon-free fuel, ammonia is a promising candidate for the future [1]. The use of ammonia has a long history, but even today, it is not a common technology and in general, it has not been considered for use as a fuel [2]. Ammonia offers several advantages as a hydrogen carrier and alternative fuel due to the absence of carbon in its molecular structure and its high volumetric hydrogen density in liquefied form [3]. It can be produced from both conventional and renewable resources, which improves its practical and economic viability [1, 3–5].

Compared to pure hydrogen, ammonia offers advantages in terms of storage and distribution safety, including easier leak detection due to its strong odor and the existence of an already established infrastructure [4]. It can also be applied in a range of energy systems, including internal combustion engines, gas turbines, and fuel cells. Existing combustion systems only need a few small changes to work with it [6]. These characteristics position ammonia as a promising energy vector to decarbonize the energy sector and to increase market adoption of hydrogen-based technologies.

*Corresponding Author
E-mail Adress: gulsan@itu.edu.tr

Submitted: 26 December 2024; **Accepted:** 12 May 2025

This paper was recommended for publication in revised form by Editorin-Chief Ahmet Selim Dalkılıç

Although ammonia has many advantages over other hydrocarbon fuels and hydrogen, it also faces certain challenges. The limited understanding of the NH_3 combustion characteristics, research gaps, methods of combustion enhancement and optimization of NO_x formation restrict the utilization of NH_3 [5]. Despite the progressive usage of ammonia in practical applications, NO_x reduction and optimization of flame stability are still main challenges [5]. The comprehensive understanding of combustion and emission characteristics are necessary for the pure ammonia and ammonia blended fuels [1, 6]. It is essential to establish a standardized methodology for comparing and verifying the reaction mechanisms. Therefore, generalized approaches should be created for determining the 'best' mechanisms for the various combustion parameters [7]. This study addresses this gap by presenting a comparative analysis of three reaction mechanisms under different operating conditions. An ammonia–hydrogen fuel blend is used to investigate the combustion behavior and to assess how accurately these mechanisms can reproduce ammonia–hydrogen combustion characteristics. Model validation against experimental temperature and emission data provides further insight into the capabilities and limitations of the considered reaction mechanisms, as well as their applicability in industrial contexts. The results also indicate that advanced numerical simulations can be used to optimize ammonia combustion systems while reducing the reliance on extensive experimental work. It facilitates the development of more efficient and sustainable energy systems by providing a detailed and validated modeling framework.

NO_x is mainly composed of thermal NO_x and fuel NO_x which is the main pollutant of ammonia combustion. Thermal NO_x is usually produced by the oxidation of N_2 at temperature up to 1800 K. Controlling the temperature is an effective way to reduce thermal NO_x production. Fuel NO_x is mainly generated by the oxidation of NH_3 and it is widely studied by researchers [6]. Ammonia does not produce NO_x as a final product when it is completely combusted and it only turns to nitrogen and water. The overall reaction of ammonia is $4NH_3 + 3O_2 \rightarrow 2N_2 + 6H_2O$ when considering the Gibbs free energy of the combustion products [8]. However, it generates relatively high NO_x emissions in practical combustion applications. Therefore, detailed reaction mechanism is required to understand and reduce the NO_x production [6].

Erdemir and Dincer [3] compared the effects of different ammonia fuel blends on the NO_x emissions. Mixing ammonia with common hydrocarbon fuels gives higher flame speeds, heat release rate and radiation intensity than pure ammonia [8].

Equivalence ratio and pressure are also important parameters for NO_x emissions. According to Kobayashi et al. [8]; burning under fuel rich condition is an effective way to reduce NO_x emission. Lee et al. [9] also found that both NO_x and N_2O emissions are low in fuel rich condition when compared to those under lean condition.

Li et al. [10] experimentally measured the NO_x concentration of NH_3/H_2/air flames, covering the NH_3 concentration from 0.440 to 0.544 at the equivalence ratios from 1.0 to 1.25. According to the results; NO_x emission decreases when the equivalence ratio increases from 1.00 to 1.25 under various NH_3 contents. The production of NO_x decreases with the increase of NH_3 concentration, which due to the low flame temperature.

Nozari et al. [11] investigated the NO_x emission variation of NH_3/H_2/air flame dependent to the equivalence ratio at 17 atm and 673 K. The NO_x concentration increased first and then decreased when the equivalence ratio changed from 0.5 to 1.2. The maximum NO_x mole fraction occurred under fuel lean conditions, similar to ammonia/air flames.

Valera - Medina et al. [12] numerically and experimentally investigated the NO_x emission of premixed NH_3/H_2 (50:50) mixtures under fuel lean condition in a swirl combustor. Pollutant emissions were higher under fuel-rich conditions.

According to the study of Franco et al. [13]; NO_x emissions increase with the addition of H_2 for a fixed equivalence ratio. For a constant fuel composition, NO_x increases with equivalence ratio up to 0.9, with a slighter increase between 0.8 and 0.9.

Xiao et al. [14] investigated the effect of pressure in NH_3/H_2 flames by using an improved reaction mechanism developed by Mathieu et al. [15]. The NO_x concentration significantly decreases with the rise of pressure.

Rocha et al. [16] numerically investigated the change of NO_x emission dependent to H_2 addition ratio by using ten mechanisms for ammonia/ hydrogen/air flames. Results show that with an increase of the H_2 content, the NO_x emission increased before the mole fraction of H_2 reached 0.8 and then rapidly decreased when the mole fraction of H_2 higher than 0.8.

According to the Li et al. [6]; one of the main challenges in the investigation of ammonia-based fuel is the validation of numerical simulations. Due to reaction mechanisms, numerical results typically over- or underpredict the observed values. Thus, developing an accurate reaction mechanism is necessary to fully understand the combustion characteristics of ammonia-based flames.

Alnasif et al. [7] reviewed the latest trends in the chemical kinetics of ammonia extensively. Various experimental results are used to validate the kinetic reaction mechanisms. The findings show that most of the reaction mechanisms perform poorly in estimating combustion characteristics such as ignition delay, laminar flame speed and NO_x emissions. The predictive performance of the mechanisms varies with the equivalence ratio, the mixing ratio, and the operating conditions. Many mechanisms for mixed-ammonia systems give reliable predictions at low hydrogen concentrations, but their predictive accuracy deteriorates gradually due to shifts in reactions at high hydrogen concentrations. This is one of the issues that require further study. A lot of work has been done to establish a kinet-

ic mechanism that precisely predicts NO_x emissions from ammonia flames under different conditions. Over the last 10 years, substantial improvements have been made in predicting combustion characteristics by improving kinetic mechanisms and reducing inconsistencies among measurements.

Alnasif et al. [17] elucidated the differences between the mechanisms for predicting NO mole fractions by studying the effects caused by the combustion of ammonia mixtures. Despite numerous efforts to improve the performance of kinetic mechanisms, consistently exhibited poor predictive ability for the NO mole fraction across all equivalence ratios.

A reduced kinetic mechanism of NH_3/H_2/Air combustion was developed by Duynslaegher et al. [18] to optimize NO_x formation and laminar flame speed. The mechanism comprises 80 reactions and 19 species at a temperature of 673.15 K, a pressure of 140 kPa, and an equivalence ratio of 0.5. It was identified that the Duynslaegher et al. [18] mechanism reproduces the experimental measurements correctly under lean conditions, but under rich conditions the results deteriorate. In these conditions, the Nakamura et al. [19] mechanism was used for a good prediction of the flame speed. According to the evaluation, the Duynslaegher et al. [18] mechanism shows poor performance when the hydrogen content exceeds 40% and tends to overestimate the response of fuels with low hydrogen content. According to Alnasif et al. [20] studies, the kinetic model formulated by Duynslaegher et al. [18] showed the greatest precision in estimating laminar flame speed measurements under atmospheric conditions for 70/30 vol% NH_3/H_2 mixture.

Nakamura et al. [19] developed a model for high temperature and highly diluted NH_3/O_2/Ar mixtures to improve the prediction of ignition delay times. According to the results, the model reported a better prediction of species as NH_3, O_2, and H_2O. They also noted that NO and N_2O profiles were well predicted in the post-flame region, but overestimated at the reaction region.

Stagni et al. [21] intended to develop a kinetic mechanism for NH_3 oxidation in their study. They covered a wide range of studies conducted under lean conditions, using both flow and jet-stirred reactors. Thus, the study covered a wide range of operating temperatures from 500 K to 2000 K. Importantly, they determined critical pathways leading to NO formation.

In a separate study, Alnasif et al. [17] aimed to determine the most accurate kinetic model to estimate experimental measurements of NO mole fractions in NH_3/H_2 (70/30 vol%) binary flames. This study evaluated 67 kinetic reaction mechanisms. Alnasif's study results showed that the kinetic model suggested by Nakamura et al. [19] has suitable predictive capabilities and precisely match experimental measurements within the specified uncertainty limits.

Munteanu and Amzaini [22] investigated the pollutant emissions of bluff-body stabilized non-premixed flames by using Siemens Star-cm+®. They examined RANS with the k-Ɛ turbulence model to validate the Sandia B4F3A flame. The GRI-MECH mechanism was used to investigate the emissions. Although some underpredictions are observed mainly for NO and CO, these results are consistent with previously reported studies.

Mauro et al. [23] performed CFD validation for Sydney bluff body burner. Converge CFD® was used in the steady state RANS simulations. The RSM-SSG and k-Ɛ turbulence models were compared for the full burner geometry. The k-Ɛ turbulence model provided the best agreement with experiments. They investigated detailed FGM and SAGE solver models coupled with 2 reaction mechanisms (CRECK and GRI-MECH 3.0). Standard and near-wall approaches were compared to validate the reactive flow.

Vigueras-Zuniga et al. [24] aimed to characterize various ammonia/methane blends and describe the effects of flame, radical formation and stability on the swirling burners. A tangential swirl burner was employed at 8 kW and a swirl number of 1.05. RANS simulation with k-w SST turbulence model was conducted by using Siemens Star-cm+®. Okafor's reduced mechanism was applied and validated using laminar burning velocity measurements. CFD results were validated against emission measurements. One-third of the burner section was used to represent the entire geometry using periodic interface boundaries. A computational grid, consisting of 4.1 million cells, was locally refined. According to the results; correlation between species (NH_3) is adequate.

Vigueras-Zuniga et al. [25] examined a numerical study to characterize ammonia combustion systems by using novel reaction models. RANS simulations via Siemens Star-cm+® were performed with 70–30 (mol%) NH_3-H_2 blend. A fixed equivalence ratio of 1.2, a swirl ratio of 0.8, and confined conditions were applied to determine the flame and species propagation at different working pressures and inlet temperatures. The analyses were conducted using the k-w SST turbulence model. Complex chemistry was employed by using a reduced kinetic mechanism developed by Okafor et al. [26]. To investigate the non-adiabatic operating conditions of the system, tests were performed in a high-pressure optical combustor and were validated against previous results. A wall temperature of 1450 K was applied, and a numerical mesh consisting of ~1.5 million cells was used for the calculations. The mesh was locally refined in the inner flame region downstream of the nozzle. One-third of the burner section, with periodic interface boundaries, was used to represent the entire geometry. CFD models were validated by using the results from Valera-Medina et al. [27], Pugh et al. [28] and Runyon et al. [29]. The study was then expanded to include high inlet temperatures, high pressures, and high flow rates under different boundary conditions. Ammonia emissions are in good agreement with those reported in previous experimental campaigns. However, predicted hydrogen concentrations are higher than measured concentrations. Simultaneously, NO emissions are overpredicted.

Mikulcic et al. [30] performed RANS simulations for methane/ammonia combustion under conditions approaching industrial ones. Three reaction mechanisms were compared using commercial CFD software AVL Fire® and their predictions on the experimental premixed swirl burner was investigated. The burner is part of the experimental rig located at the Gas Turbine Research Centre of Cardiff University and has a geometric swirl number of 1.05. In simulations, a constant temperature of 1500 K was imposed on the wall, and the outlet boundary condition was set to 100 kPa. Comparison of experimental and simulation results indicates that the San Diego mechanism predicts NO concentrations most accurately, whereas the Konnov mechanism yields the poorest predictions. However, the San Diego mechanism is the most computationally demanding because it includes nitrogen chemistry. Other species are predicted less accurately. Comparison of the presented mechanisms shows that the San Diego mechanism is distinct from the other two in all respects, including the velocity field. It is the most promising mechanism, particularly with respect to NO emissions.

In the study by Sudarma et al. [31], lean premixed combustion in a bluff-body stabilized burner was numerically investigated. The k-ε and RSM turbulence models were compared with and validated against experimental data. While the k-ε model provided better overall flame predictions, the RSM approach proved to be more accurate in capturing local flow structures. This highlights the importance of choosing an appropriate turbulence model in combustion simulations.

Muppala et al. [32] carried out a comparative study of several turbulent reaction models for hydrogen-enriched methane-air flames. Their results show that traditional models often fail to capture combustion behavior at high hydrogen fractions, mainly because of diffusion-related effects becoming more dominant.

In a similar direction, Rajak et al. [33] used CFD-based models to investigate combustion characteristics and NOx emissions for different gaseous fuels, including hydrogen-air mixtures. Their findings indicate that fuel type, flame temperature, and radiative heat transfer play a key role in NO formation. The model was also validated using experimental data, particularly for NO concentration trends.

More recently, ammonia has gained attention as a potential clean fuel, although it still presents several challenges in practical applications. These include low flame speed, long ignition delay, and emission issues such as NO_x formation and unburned ammonia in the exhaust gases [34]. To address these limitations, different strategies have been proposed, including staged combustion, exhaust gas recirculation, and selective catalytic reduction systems. In addition, research has increasingly focused on improving burner designs and fuel blending strategies, particularly for use in gas turbines, internal combustion engines, and industrial boiler systems.

Based on these findings, this study evaluates the performance of various reaction mechanisms in an industrial-scale burner fueled with an ammonia–hydrogen blend under both rich and lean combustion conditions. The goal is to provide useful insights for developing cleaner and more efficient combustion systems.

2. Experimental setup

This study used the burner geometry and related experimental data available from the Gas Turbine Research Centre (Port Talbot, Wales), a research facility of Cardiff University. Figure 1 illustrates the burner setup. Further details can be found in other sources [35-38].

A tangential swirl burner at an industrial scale, characterized by a geometric swirl number of S_g=1.05, was examined. Figure 2 shows a detailed geometric view of the burner. Fuels and air exit the premix chamber (label a) through the burner nozzle (r = 28 mm) via a single radial-tangential swirler (label b); the central injection lance (label c) serves as a bluff body (r = 16 mm). The flame was contained within a cylindrical quartz enclosure (label d), which had an expansion ratio of 3 relative to the burner's exit nozzle. A honeycomb (label e) was implemented to reduce the risks linked to flashback and to homogenize the flow [38].

The burner was provided with Bronkhorst controllers for mass flow (±0.5% within a range of 15–95% mass flow).Air and NH_3 are injected at the mixing chamber, while the H_2 is injected from the 6 equispaced holes those have 1.5 mm diameter. They are located 4 cm below the burner exit, angled at 45°, give H_2 into the swirler directly for premixing with ammonia and air [35-37, 39]. Quartz material was used at the burner walls for the optical access [37].

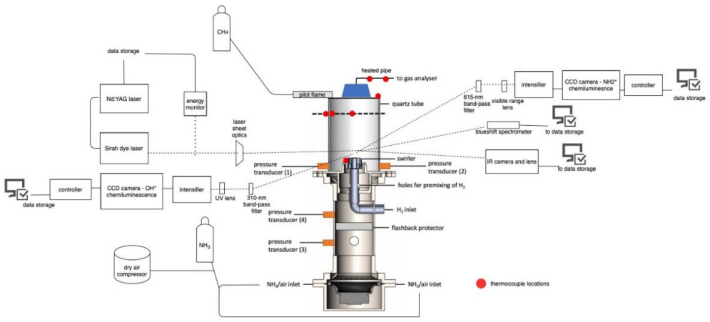

Figure 1. Tangential combustor with measuring techniques and control systems [open access, 35]

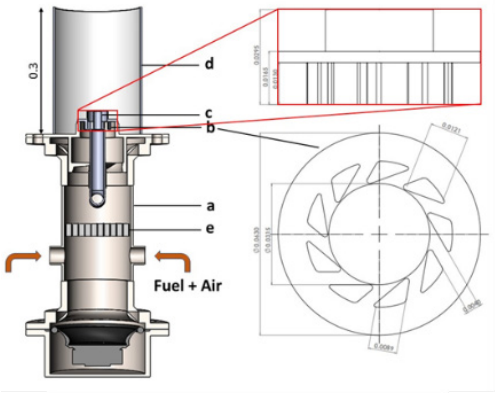

Figure 2. Detailed geometrical view of the burner. Dimensions in meter(m)[open access, 38]

Time-averaged flame images were obtained with two simultaneously operating intensified cameras [35]. For each case, 500 frames were collected using LaVision Davis v10. Abel deconvolution was applied to the time-averaged data after a 3x3-pixel median filter. Chemiluminescence images were normalized to their peak intensities in the colour maps to illustrate the variations in species distributions across each flame. The results for the measured species are presented in the Results chapter (Figures 9, 11, and 13). Temperature profiles were measured using K- and R-type thermocouples connected to a data logger at a sampling frequency of 1 Hz. Thermocouple data were collected at each point for 120 s and then averaged. The thermocouples were calibrated with an average error of 3%. The collected temperature data were corrected according to [40] to account for conductive heat transfer between the thermocouple bead and the connecting thermocouple wires, and radiative and convective heat transfer between the thermocouples and their surroundings. A custom quantum cascade laser analyzer with a sampling frequency of 1 Hz(±1%, 0.999 linearity)and operating at 463 K was used to measure exhaust emissions consisting of NO, NO_2, N_2O, NH_3, H_2O and O_2. An isokinetic funnel, with an inlet diameter of 30 mm, was positioned 50 mm above the outlet of the quartz restriction to obtain homogeneous exhaust samples under the specified operating conditions. A heated line at 433.15 K was used to obtain exhaust samples and prevent condensation [37]. All emission data were collected for 120 s and averaged. The emission data provided here are normalized to a reference of 15% O_2 [41].

The dilution methodology was presented by adding N_2 to the sample [37]. A Bronkhorst EL-FLOW Prestige MFC with high sensitivity was used in this process. Before mixing with the exhaust samples, N_2 is heated by the system to 433.15 K. The flow meter in the analyzer, calibrated by the manufacturer, is sufficient for its intended purpose. Equation (1) calculates the sample flow rate from the system's exhaust during the dilution procedure. The repeatability in this dilution methodology is ±10%. This methodology is applied when wet readings exceed the analyser's detection range.

$$F_s = F_{t,i} - F_{d,N_2} \quad (1)$$

Temperatures at multiple locations and exhaust emissions were measured for 6 cases. Three power levels were investigated for both the rich (equivalence ratio 1.2) and the lean (equivalence ratio 0.7) conditions. The equivalence ratio was adjusted by changing the airflow while keeping the fuel flow rate constant. The cases and test parameters are given in Table 1.

Table 1. Simulated cases

		NH_3		H_2		Air			
Case Number	NH_3/H_2 (vol.%)	Vol. flow rate (dm^3/s)	Mass flow rate (g/s)	Vol. flow rate (dm^3/s)	Mass flow rate (g/s)	Vol. flow rate (dm^3/s)	Mass flow rate (g/s)	Equivalence ratio (Φ)	Power (kW)
1	50/50	0.850	0.613	0.850	0.073	4.233	5.168	1.2	20
2	50/50	0.850	0.613	0.850	0.073	7.257	8.86	0.7	20
3	50/50	0.638	0.460	0.638	0.0545	3.178	3.881	1.2	15
4	50/50	0.638	0.460	0.638	0.0545	5.450	6.653	0.7	15
5	50/50	0.425	0.306	0.425	0.0363	2.117	2.584	1.2	10
6	50/50	0.425	0.306	0.425	0.0363	3.628	4.43	0.7	10

3. Numerical model

Converge CFD® [42] was used for the numerical simulation of the swirl burner. Figure 3 shows the surface-meshed 3D model. To minimize the computational cost, the burner geometry was modeled as a 1/3 slice using periodic boundary conditions. The axial length of the burner was extended by 30 mm beyond the outlet surface to accurately simulate the experiments and to prevent numerical errors that may arise from boundary conditions. Additionally, the extended outlet volume corresponds to the exhaust-gas sample used for emission analysis during experiments. Therefore, it was used to calculate numerical emissions based on the simulation results. The

inlet surfaces were defined by a constant mass flow rate (Table 1) and a gas temperature of 288 K, whereas the outlet surface was assumed to be at atmospheric conditions. All burner and swirler walls are defined as adiabatic, with no-slip boundary conditions. A transient RANS model was employed with adaptive mesh refinement to address critical regions, particularly near the swirler.

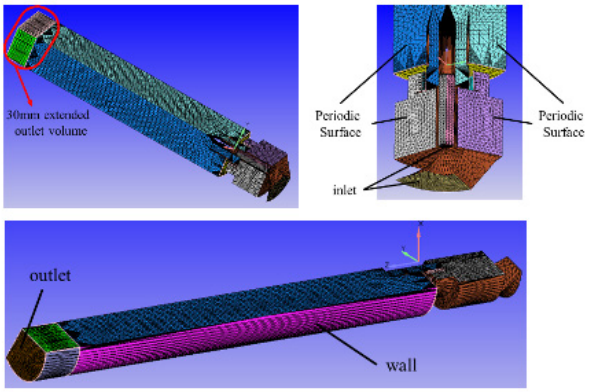

Figure 3. Surface meshed burner model

Figure 4 represents the AMR controlled volume mesh structure of the model with 1.2 million cells generated in Converge CFD®. The cell's base grid size is set to 4 mm, with a maximum of 3 embedding levels for temperature AMR, and a 3K sub-grid criterion. A 0.05 m/s velocity sub-grid criterion was applied to the inlet and swirler regions, while other regions used a 0.2 m/s velocity sub-grid criterion. All domains have a maximum embedding level of 4 for velocity AMR. The surface of the swirler vanes was improved with a 2-embedded layer and a 5-scale fixed embedding. 2 embedding layers were added to the inner surfaces of the nozzle holes, and a fixed 4-scale embedding was also applied. As a final mesh refinement, the lower axial half of the domain was subjected to a 1-scale fixed embedding. With this meshing strategy, all critical zones are captured accurately, over-meshing is avoided, and total computational time is reduced. Readers interested in the adaptive meshing technique and its definitions are referred to [42] for further details.

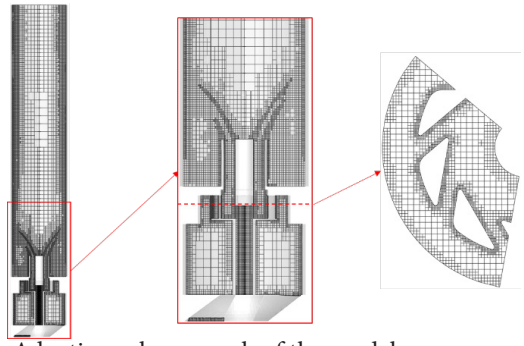

Figure 4. Adaptive volume mesh of the model

The coldflow validation of this burner is performed at previous study [43]. Gulsan and Boke [43] compared six different turbulence models both for the first and second order solvers to obtain the most proper model with the LDA experiments. Based on the comparison of axial velocity profiles at various axial positions, the second-order k-ω SST turbulence model was selected as the best match to the experimental results (Figure 5). It is consistent with previous studies [24, 25, 44-46] that have used k-w SST turbulence model in similar burner simulations. Also, the one of them [46] has an additional turbulence model comparison that chooses k-w SST for the tangential swirling flows. Once the isothermal profiles were validated, the numerical model was modified to investigate reacting flow.

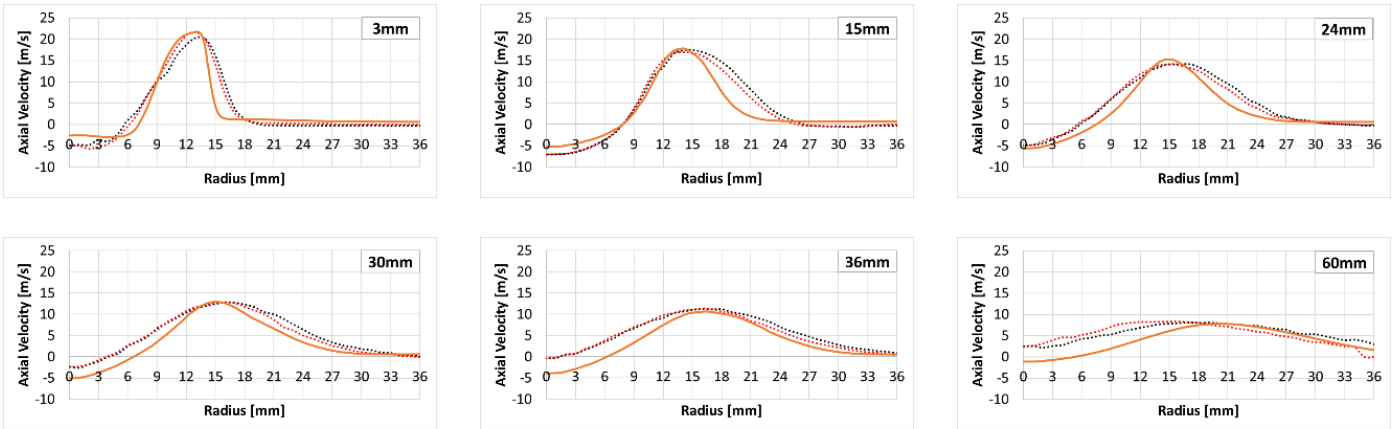

Figure 5. Comparison of velocity profiles at various axial positions. LDA experiments (dashed red line-right side, dashed black line-left side) and numerical (solid orange line)[43]

According to the absolute percentage error analysis performed by Alnasif et al. [20]; Duynslaegher et al. [18], Nakamura et al. [19] and Stagni et al. [21] were selected as candidate mechanisms for the numerical simulations in this study (Table 2). The summary of the study's boundary conditions and parameters is presented in Table 3.

Table 2. Compared reaction mechanisms

No	Reaction Mechanism	Number of Reactions	Number of Species
1	Duynslaegher [18]	80	19
2	Nakamura [19]	232	33
3	Stagni [21]	210	31

Table 3. Boundary conditions and parameters

Parameter	Value
Quartz Wall Temp	Adiabatic
Burner Section	Symmetry (120°)
Swirler Walls	Adiabatic
Inlet Boundary Condition	Table 1
Inlet Temperature	288 K
Inlet Pressure	110 kPa
Outlet Pressure	Atmospheric P

Parameter	Value
Blend	50-50 NH_h-H_2 (vol%)
Mixing	Fully Pre-Mixed
Equivalence Ratios	0.7 and 1.2
Power	10/15/20 kW
Turbulence Model	k-w SST
Walls	No-Slip
Swirl	1.05

Simulations were performed with SAGE detailed chemistry solver by using 50-50(vol%)NH_3-H_2 blend. Six different experimental cases (Table 1) were simulated with Duynslaeger et al. [18], Nakamura et al. [19] and Stagni et al. [21] mechanisms to obtain the most appropriate model.

4. Results

The results of the numerical model were compared with experimental measurements to validate the reacting flow. The temperature values and exhaust species produced by the reaction mechanisms were investigated via simulations to select the most appropriate model. The thermocouple locations are shown in Figure 1. Temperature data taken from four thermocouple locations (Figure 6) were compared with the CFD results in Figure 7.

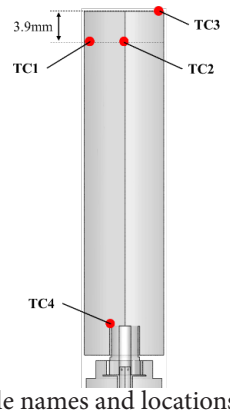

Figure 6. Thermocouple names and locations

In the experiments, thermocouple TC1, located 3.9 mm inside the burner exit, recorded lower temperatures in the rich cases (1-3-5) than in the lean cases (2-4-6). Depending on the fuel flow, the temperature at TC1 decreases from case 1 to case 6. For cases 2 and 4, the numerical errors are below the measurement error, and all mechanisms are in excellent agreement with the experimental data. Stagni et al. [21] overpredicts at the case 3 and Nakamura et al. [19] underpredicts at the case 6; although the Duynslaeger et al. [18] have valid results for both cases. Numerical errors are significant only for rich cases 1 and 5. Although the percentage of errors are close to each other; Nakamura et al. [19] gives the best results with experiments at case 1 and case 5. Compared with rich cases (1-3-5), CFD results for lean cases (2-4-6) are much closer to experimental measurements, independent of the mechanism. While errors in numerical models are lower(4%)under lean conditions, they increase to nearly 9% under rich conditions.

For the thermocouple TC2 which at the center of the burner exit; all of the CFD results give lower errors (≤5%) with the experiments. Rich cases (1-3-5) exhibit good accuracy across all mechanisms; all errors are below the thermocouple reading error. At the lean cases (2-4-6); Nakamura et al. [19] and Stagni et al. [21] have better results compared to Duynslaegher et al. [18]. The lean experiments exhibit higher temperatures than the simulations.

For TC3, the thermocouple temperature is higher under lean conditions than under rich conditions. Stagni et al. [21] mismatches with experiments both for the rich and lean conditions especially at cases 2, 3 and 4. Although the Duynslaegher et al. [18] gives better results than Stagni et al. [21]; this mechanism gives higher variances with experiments. Compared to these two mechanisms, Nakamura et al. [19] represents the TC3 temperature better.

Similar to TC2, the temperature decreases under lean conditions in TC4. The errors were nearly 18% in cases 2 and 6. Nakamura et al. [19] has the highest overprediction at the cases 1 and 4. Although it has very high errors at case 2 and 5; Stagni et al. [21] has the good results for other cases. Although the results for each mechanism are challenging to interpret, there is no physical correlation between the temperature values and combustion parameters.

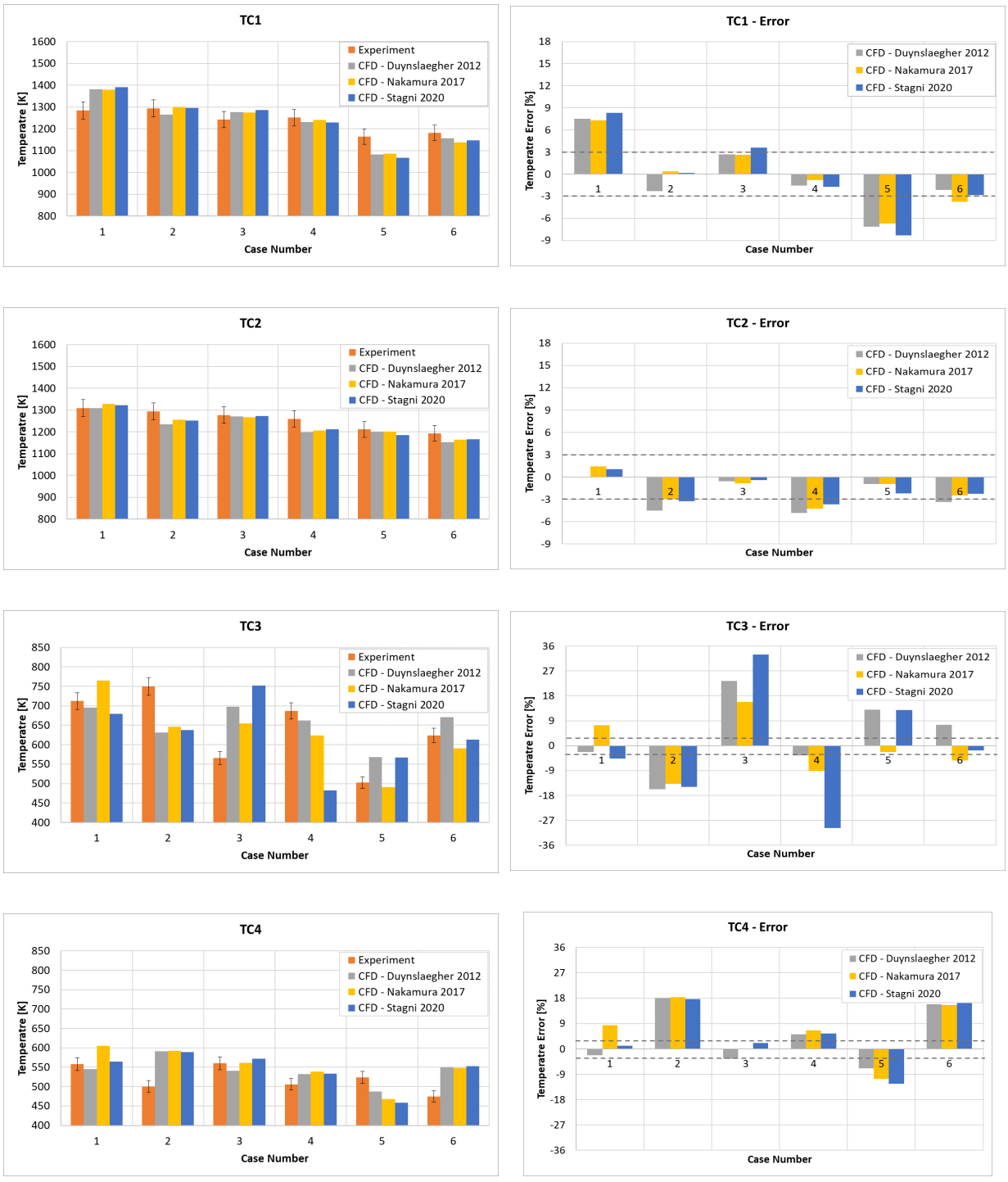

Figure 7. Comparison of temperature data at various burner locations

Figure 8 presents the temperature distribution from the simulations for each case. Independent of the reaction mechanism, the average burner temperature is lower in the rich cases (1, 3, and 5), except in Duynslaegher Case 1 and Case 2. As airflow increases, regions of maximum temperature shrink. Compared to the other two mechanisms, Duynslaegher et al. [18] exhibit lower mixing-zone temperatures, especially for the first three cases. It also exhibits higher local temperatures in the last three cases. Nakamura et al. [19] and Stagni et al. [21] mechanisms have similar trends at all of the cases.

These temperature differences reflect how each mechanism handles ammonia-hydrogen combustion under different conditions. Duynslaegher [18] mechanism was developed for low temperature conditions and predicts lower flame temperatures, especially for lean mixtures. This may be due to slower NH_3 oxidation rates [7]. Nakamura [19] provides better results in rich conditions, where fuel-N conversion is more dominant and oxygen availability is limited [17]. Furthermore, the overall lower flame temperatures observed in rich cases are consistent with earlier studies, which associate fuel-rich combustion with incomplete oxidation and reduced adiabatic flame temperature [8].

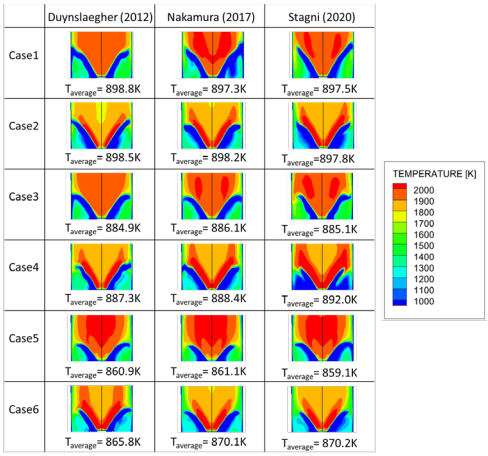

Figure 8. Temperature distributions of simulated cases

On the experimental studies; the OH, NH and NH_2 species were measured with chemiluminescence. Images were normalized to the maximum value in each image to illustrate differences between species.

Figure 9 shows the OH distributions obtained in the experiments. The maximum OH generation occurs at the stagnation points around the recirculation zone. In rich cases (1, 3, and 5), as the flow rate decreases, and depending on the stagnation point of the recirculation zone, the OH-generation region relocates from the liner walls to the center of the burner. In contrast to the rich cases, the max OH concentration is observed at the center of the burner under lean conditions (2-4-6). No region near the liner walls exhibits a higher OH value. Due to the higher flow rates under lean conditions, stagnation points, which generate higher OH concentrations, disappear from the recirculation zone.

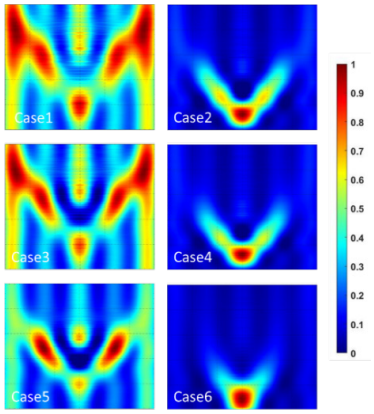

Figure 9. Oh distribution of experiments

Figure 10 also shows the OH distributions from the simulations. The models successfully reproduce the OH distribution for the rich cases(1, 3, and 5).All three mechanisms produce similar results. The lean conditions(2, 4, and 6)produce higher OH levels, with the maximum observed in condition 4. Duynslaegher et al. [18] follows a different pattern at lean cases while other mechanisms are similar. Since the tendency of lower OH at Case 2; Nakamura et al. [19] one step closer to the experimental measurement.

The OH distribution is strongly influenced by the flow structure, especially the central recirculation zone created by the swirling flow. Under lean conditions, excess oxygen leads to increased OH formation along the centerline. This agrees with previous studies showing that lean flames are more oxidizing [8]. Under rich conditions, OH is distributed more toward the sides. This is likely due to fuel stratification and limited oxygen near the center. Although all three mechanisms show similar general trends, Nakamura [19] gives the best agreement with the experimental OH profiles, especially in terms of intensity and spatial distribution.

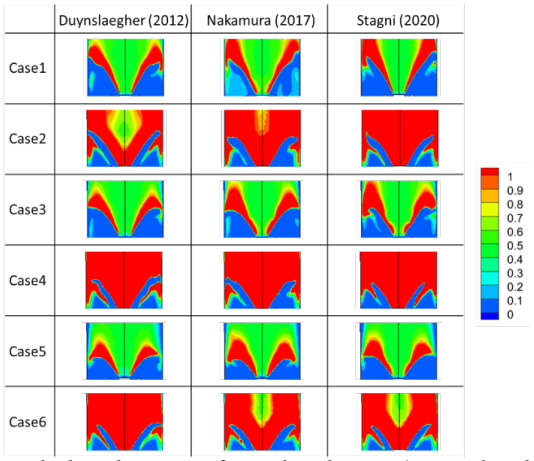

Figure 10. Oh distributions of simulated cases (normalized with max 5.0e-4 mole fraction)

Figure 11 shows the NH distribution of chemiluminescence measurements. The trend in NH distribution is very similar to that of

OH under lean conditions (2-4-6). The maximum NH is observed at the center of the burner. For the rich cases (1, 3, and 5), critical zones coincide with the OH distribution. However, the liner walls show higher NH values as the power of the burner decreases, contrary to the OH distribution. When compared with simulations (Figure 12); only the Stagni et al. [21] gives similar distribution with experiments under rich conditions. The NH distribution of Nakamura et al. [19] is different from the measurements and Duynslaegher et al. [18] has more NH than other mechanisms. For the lean conditions; Nakamura et al. [19] and Stagni et al. [21] have similar trends.

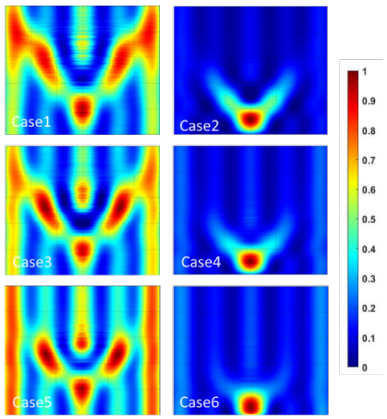

Figure 11. Nh distribution of experiments

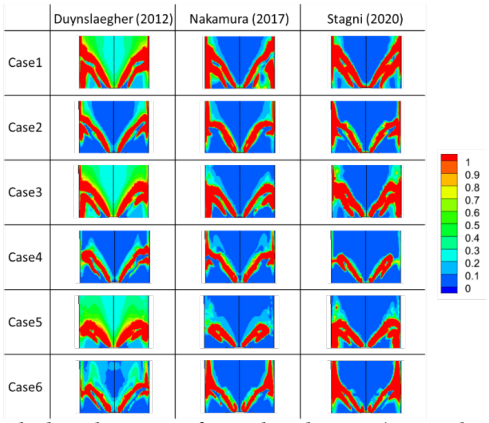

Figure 12. Nh distributions of simulated cases (normalized with max 3.0e-7 mole fraction)

NH_2 distributions are not same for the experiments and simulations (Figure 13 and Figure 14). The max NH_2 is seen around the recirculation zone under rich conditions. It spreads to the center of the burner when the power level decreases. This trend is also seen in the rich case simulations. Under lean conditions; the maximum NH_2 is seen at the center of the burner. Although it diffuses towards the walls, it moves to the center as power decreases. This phenomenon is also seen in the lean simulations. Duynslaegher et al. [18] generates higher NH_2 for all the cases when compared with other two mechanisms. At the rich cases (1-3-5); Stagni et al. [21] generates more NH_2 than Nakamura et al. [19]. In contrast to it; Nakamura et al. [19] gives higher values than Stagni et al. [21] at lean conditions (2-4-6). Although there is not a powerful correlation between the experiments and simulations; Nakamura et al. [19] and Stagni et al. [21] are more appropriate candidates for the validation.

The formation of NH and NH_2 radicals is significantly influenced by the equivalence ratio. Under rich conditions, where oxygen is limited, the simulations show higher NH_x concentrations. This trend is consistent with previous studies reporting that fuel-derived intermediate species remain at higher levels under incomplete combustion conditions [10]. Among the evaluated mechanisms, Stagni [21] gives the closest agreement with the experimental NH profiles in these cases, which may be related to its relatively slower oxidation rates of nitrogen-containing radicals. In lean mixtures, both Nakamura [19] and Stagni [21] predict centrally located NH_x peaks, possibly due to enhanced post-flame oxidation resulting from the increased oxygen availability. This behavior is consistent with the expected chemical shift from intermediate nitrogen species toward final products such as NO or N_2 in fuel-lean flames.

NO, NO_2 and NH_3 measurements were performed with gas analyzer. In Figure 15, the NO emissions increase for the rich cases (1, 3, and 5), while the power level decreases. In the lean cases (2, 4, and 6), NO concentrations were measured up to 1000ppmV, but further measurements could not be taken because the analyzer's detection limit was reached. The trend in rich cases may also be observed in lean cases when measured with appropriate tools. Up to that time, it can only be said that the NO levels in lean cases are higher than in rich cases (1-3-5). According to the CFD simulations, all compared mechanisms show the same trend as observed in experiments. Except the case 1; Duynslaegher et al. [18] have the worst approximation with NO measurements. Stagni et al. [21] is better than Duynslaegher et al. [18], but Nakamura et al. [19] gives the best matching especially at the rich cases.

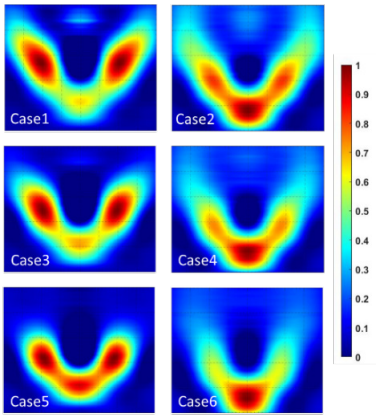

Figure 13. NH_2 distribution of experiments

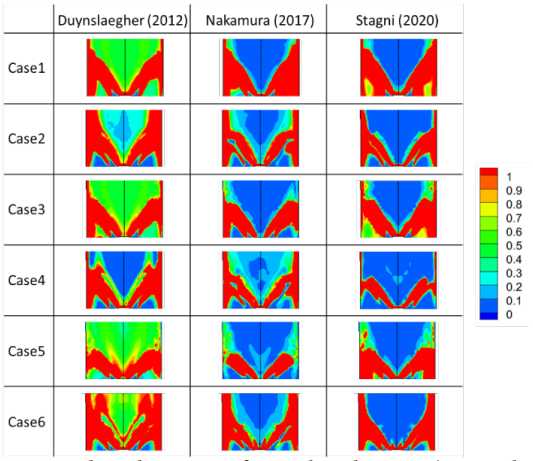

Figure 14. NH_2 distributions of simulated cases (normalized with max 1.0e-6 mole fraction)

NO_2 production is excessive at lean cases (2-4-6) and they were measured with the dilution as explained in the experimental setup section. In contrast, in rich cases (1-3-5), it could not be measured because of the low production level. Therefore, no experimental data are available for these cases. The evidence of low NO_2 production is CFD results also (Figure 16). All of the rich cases have very low NO_2 levels compared to lean cases. All reaction mechanisms perform well in case 4. Duynslaegher et al. [18] and Stagni et al. [21] have higher errors compared to Nakamura et al. [19] both for the case 2 and 6.

Since the degree is different between the rich and lean cases; NH_3 measurements are presented with two graphs at Figure 15. The rich cases (1-3-5) are beyond the analyzer measurement ability, therefore their NH_3 values are limited around the 530 ppmV. Stagni et al. [21] gives the nearest results at rich cases with max 25% error at case 3. With the 70% maximum error at case 3; Nakamura et al. [19] has the highest error values at all of the rich cases. Duynslaegher et al. [18] has around 40% error independent from the power level of rich cases. Although it is the best choice for the rich conditions; Stagni et al. [21] is the worst option for the lean conditions (2-4-6) when compared with experimental results. Similar to this contraction; Nakamura et al. [19] gives the most accurate NH_3 expectation under lean conditions. Duynslaegher et al. [18] is an unresponsive reaction mechanism that gives the same error level independent from the power level of burner.

Similar to Figure 15; Duynslaegher et al. [18] have the lowest NO contour compared to other two mechanisms at Figure 17. Nakamura et al. [19] and Stagni et al. [21] give very similar results under lean conditions (2-4-6). However Nakamura et al. [19] closes to experiments for the rich cases (1-3-5).

Figure 16 shows no significant differences between mechanisms under rich conditions. Also, the experimental data are not available. Therefore, it cannot be compared with the rich cases (1-3-5). Duynslaegher et al. [18] has different results under lean conditions. Although the Stagni et al. [21] and Nakamura et al. [19] have close distributions; Nakamura et al. [19] gives the better validation with measurements.

NO formation is observed to be higher under lean conditions, which is consistent with elevated flame temperatures and increased concentrations of OH radicals—key drivers in the oxidation of fuel-bound nitrogen [17]. This trend is consistent with the general understanding that thermal and prompt NO formation increase under oxygen-rich, high-temperature conditions. Among the evaluated models, Nakamura [19] shows the closest agreement with the experimental NO results in rich flames, possibly because it represents intermediate species and fuel-N to NO conversion reactions in more detail. For NO_2, which forms primarily through the post-flame oxidation of NO, levels are considerably higher under lean conditions, where excess oxygen is available. Nakamura [19] again predicts this behavior more accurately, particularly at moderate thermal loads, likely due to its inclusion of extended NOx sub-mechanisms and post-flame chemistry.

Figure 18, similar to the experimental results, shows a major difference between the rich and lean cases. Although it is not the best at any cases; Duynslaegher et al. [18] represents the NH_3 with about 40% error for any case. Stagni et al. [21] perfectly matches the rich cases (1-3-5), but it significantly underpredicts the lean cases (2-4-6). In contrast to it; Nakamura et al. [19] is the best mechanism for the lean cases (2-4-6) but it overpredicts the rich cases (1-3-5).

NH_3 emissions are higher under rich conditions due to incomplete oxidation resulting from limited oxygen availability. The presence of unreacted ammonia in these cases is consistent with previous NH_3/H_2 combustion studies, which have also reported increased ammonia slip under fuel-rich conditions [17]. Among the evaluated mechanisms, Stagni [21] gives the closest prediction of NH_3 levels in rich flames, which may be attributed to its comparatively more conservative ammonia conversion behavior. On the other hand, Nakamura [19] tends to overpredict NH_3 under rich conditions, although it shows better agreement with experimental results in lean operation. These variations underline the importance of selecting an appropriate reaction mechanism, particularly when accurate prediction of fuel conversion and emission characteristics is required.

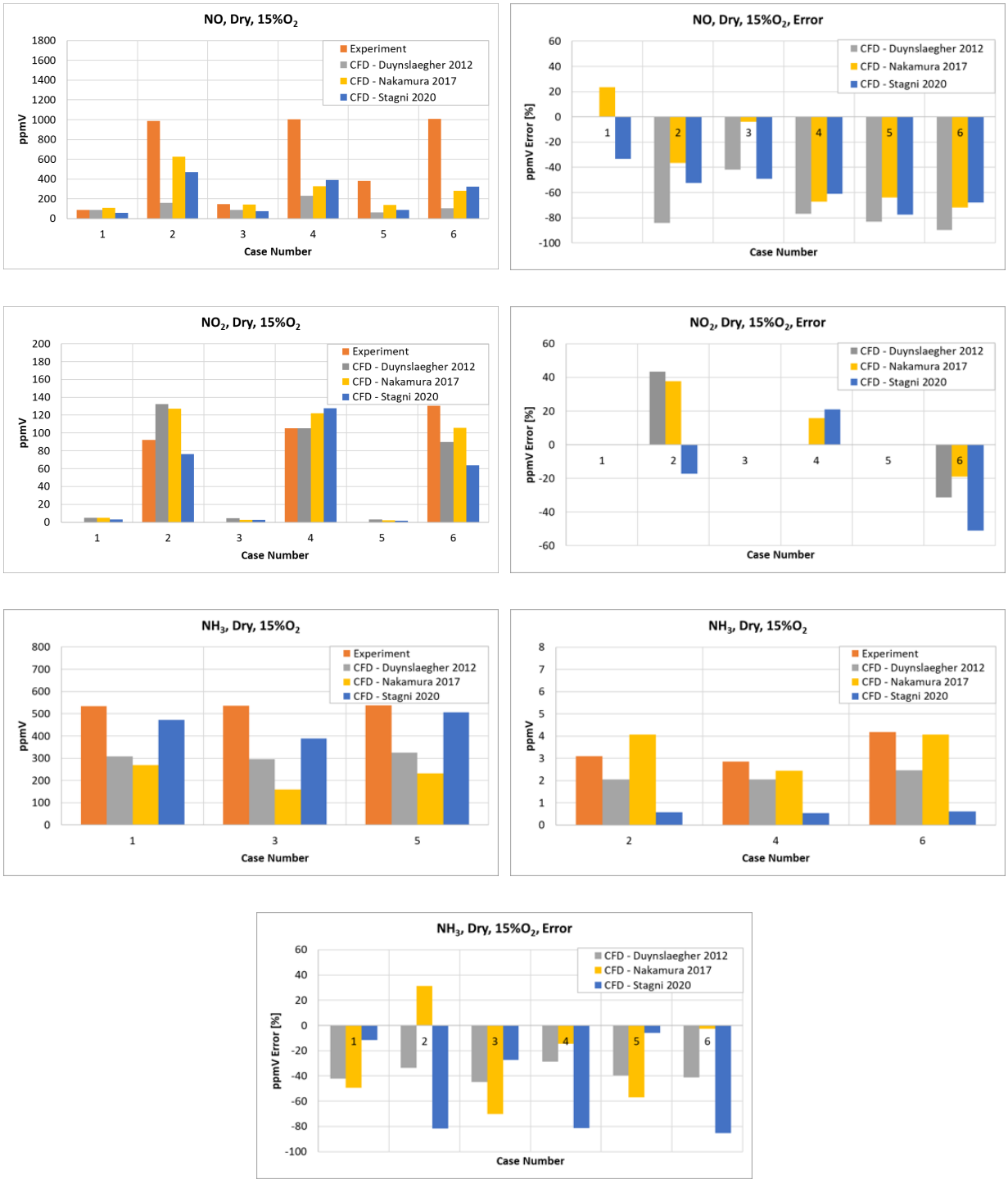

Figure 15. The comparison of reaction mechanisms with experiments for the exhaust emissions

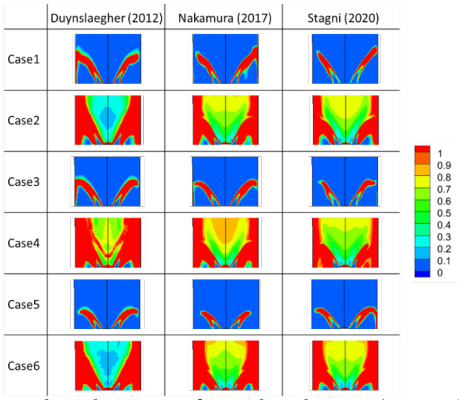

Figure 16. NO_2 distributions of simulated cases (normalized with max 1.0e-5 mole fraction)

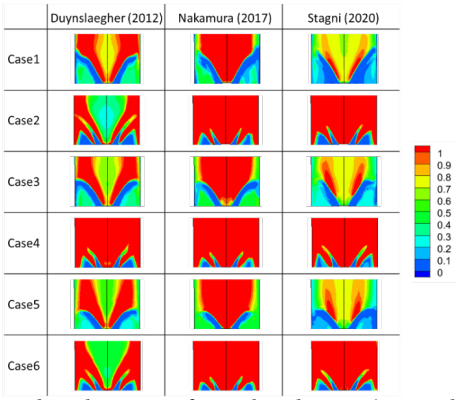

Figure 17. NO distributions of simulated cases (normalized with max 3.0e-3 mole fraction)

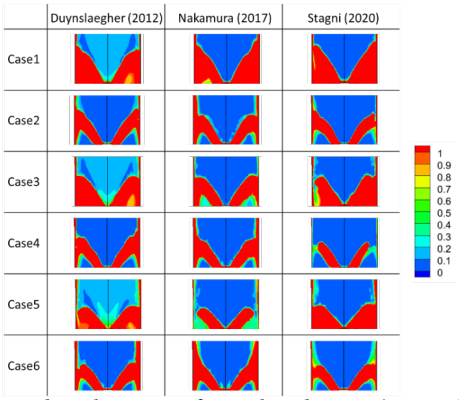

Figure 18. NH_3 distributions of simulated cases (normalized with max 1.0e-3 mole fraction)

5. Conclusion

Ammonia could be a key solution for reducing carbon emissions by enabling the transition of hydrocarbon combustion systems to hydrogen-based alternatives. Although pure hydrogen is considered an ideal carbon-free fuel, several technical challenges limit its widespread application. In this context, ammonia can be considered an effective hydrogen carrier as well as an alternative fuel. It may be utilized directly, partially decomposed, or blended with other fuels. These approaches provide practical advantages for decarbonizing energy systems and support the implementation of hydrogen-based combustion technologies.

Considerable research has been carried out to improve the combustion characteristics of ammonia, both in its pure form and in fuel blends. However, developing a kinetic mechanism that can accurately represent all combustion processes across different equivalence ratios, fuel mixture compositions, and a wide range of operating conditions remains a significant challenge. Existing reaction mechanisms tend to show varying levels of accuracy depending on the operating conditions, suggesting that each one is more suitable for specific cases. For this reason, comparative analyses of different reaction mechanisms are necessary in order to properly validate numerical models against experimental data.

In this study, an industrial-scale swirl burner operating with a 50-50 ammonia-hydrogen fuel blend by volume was numerically investigated. Three reaction mechanisms—Duynslaegher, Nakamura, and Stagni— were compared at power levels of 10, 15, and 20 kW and equivalence ratios of 1.2 and 0.7. Experimental temperature and exhaust emission data were used to determine the most appropriate mechanism for these conditions. The temperature results (Figures 7-8) indicate that the Nakamura et al. [19] mechanism provides the most comprehensive predictions. To further validate this conclusion, exhaust-emission measurements and the spatial distributions of chemiluminescence from OH, NH, and NH_2 were investigated. Nakamura et al. [19] exhibited the closest match to experimental distributions, with Stagni et al. [21] as the second-best alternative. As a last indicator; Nakamura et al. [19] aligned most accurately with gas analyzer results (Figure 15), compared to Stagni et al. [21] and Duynslaegher et al. [18]. Although experimental species distributions were not available, simulated distributions of NO, NO_2, and NH_3 were presented to highlight the differences between the mechanisms. The observed discrepancies, particularly for NO and NO_2, are mainly related to how nitrogen chemistry is represented in each mechanism, including differences in fuel-bound nitrogen conversion and post-flame oxidation pathways. Nevertheless, inconsistencies between numerical predictions and experimental data still remain, especially for NO_2 and NH_3. In this regard, Nakamura et al. [19] appears to be the most suitable mechanism for this study, more detailed and refined mechanisms will be necessary for future numerical investigations. Future work should focus on improving nitrogen sub-mechanisms by validating them with broader experimental datasets. Special attention should be given to pressure and temperature dependent reaction pathways in order to improve the prediction accuracy of NO and NO_x emissions.

Although the present study establishes a validated numerical framework for the ammonia-hydrogen swirl burner, several limitations remain. Future studies should consider more comprehensive reaction mechanisms that can represent ammonia combustion over a wider operating range. In addition, recent developments in AI may

help in incorporating complex chemical mechanisms into high-fidelity 3D numerical simulations. This could enable more extensive use of advanced approaches such as LES, DNS, and hybrid models, which in many cases offer improved accuracy compared to conventional RANS formulations. Once properly validated, such numerical models can be employed to optimize burner designs while reducing reliance on extensive experimental campaigns, thereby lowering overall development costs. In the longer term, reliable simulations may also support the transition from fossil-fuel-based systems to ammonia-fueled technologies, contributing to the decarbonization of energy production.

Overall, this study provides a validated numerical framework for ammonia–hydrogen swirl burners. The proposed framework can be useful for the design of industrial combustion systems, including boilers and heating applications. Improved predictions of temperature fields, combustion efficiency, and NOx formation allow for a more consistent evaluation of emission control strategies.

In particular, accurate NOx prediction remains critical for meeting environmental regulations without compromising combustion stability. Ammonia-based combustion systems also appear promising for gas turbine and power generation applications, where emission reduction requirements must be carefully balanced with efficiency considerations.

Furthermore, the validated numerical approach allows the assessment of ammonia combustion coupled with waste heat recovery and advanced thermal management strategies. Overall, the proposed modeling framework supports the systematic optimization of ammonia-based energy systems.

Acknowledgement

The authors gratefully acknowledge Professor Agustin Valera-Medina and Dr. Syed Mashruk for providing the experimental data prior to this study.

Authorship contributions

Mehmet Anil Gulsan: Writing- Original draft preparation, Investigation, Methodology, Validation, Editing Conceptualization and Visualization. Yakup Erhan Boke: Supervision and Reviewing.

Data availability statement

The authors confirm that the data supporting the findings of this study are available in the article. Raw data that support the findings of this study are available from the corresponding author upon reasonable request.

Conflict of interest

The author declares no potential conflicts of interest with respect to the research, authorship, and/or publication of this article.

Ethics

There are no ethical issues with the publication of this manuscript.

Funding

The authors confirm that no funding was received for this research.

Copyright and permission statement

All figures included in this manuscript are the authors' original work. Figure 1 and Figure 2 used in this manuscript have been obtained from an Elsevier article under the terms of open access and are used in accordance with the applicable licensing conditions.

Nomenclature

F	Flow rate, kg/s
FGM	Flamelet generated manifold
GRI	Gas research institute
HVAC	Heating, ventilating and air conditioning
LDA	Laser doppler anemometry
LES	Large eddy simulation
ppmV	Parts per million by volume
P	Pressure, kPa
r	Radius, mm
RANS	Reynolds averaged navier-stokes
RSM	Reynolds stress model
S	Swirl number, nd
SAGE	Stochastic acceleration by gradient estimation
SSG	Speziale-sarkar-gatski
SST	Shear stress transport
T	Temperature, K

Greek symbols

Φ	Equivalence Ratio, nd

Subscripts

d	Refers to dilution
g	Refers to geometric
i	Refers to inlet
N_2	Refers to
s	Refers to exhaust gas sample
t	Refers to total

References

[1] Ishikawa, Y., Hayashi, J., Takeishi, H., Okanami, T., Yamamoto, Y., Iino, K., & Akamatsu, F. (2018).Study on flame stability in oxygen-enriched ammonia/N_2/O_2 laminar diffusion flame. Transactions of the JSME(in Japanese), 84(859). https://doi.org/10.1299/transjsme.17-00526

[2] Hayakawa, A., Arakawa, Y., Mimoto, R., Somarathne, K. D. K., Kudo, T., & Kobayashi, H. (2017). Experimental investigation of stabilization and emission characteristics of ammonia/air premixed flames in a swirl combustor. International Journal of Hydrogen Energy, 42(19),14010–14018. https://doi.org/10.1016/j.ijhydene.2017.01.046

[3] Erdemir, D., & Dincer, I. (2020). A perspective on the use of ammonia as a clean fuel: Challenges and solutions. International Journal of Energy Research, 45(4),4827–4834. https://doi.org/10.1002/er.6232

[4] Herbinet, O., Bartocci, P., & Grinberg Dana, A. (2022). On the use of ammonia as a fuel – a perspective. Fuel Communications, 11, 100064. https://doi.org/10.1016/j.jfueco.2022.100064

[5] Elbaz, A. M., Wang, S., Guiberti, T. F., & Roberts, W. L. (2022). Review on the recent advances on ammonia combustion from the fundamentals to the applications. Fuel Communications, 10, 100053. https://doi.org/10.1016/j.jfueco.2022.100053

[6] Li, J., Lai, S., Chen, D., Wu, R., Kobayashi, N., Deng, L., & Huang, H. (2021). A review on combustion characteristics of ammonia as a carbon-free fuel. Frontiers in Energy Research, 9, 760356. https://doi.org/10.3389/fenrg.2021.760356

[7] Alnasif, A., Mashruk, S., Shi, H., Alnajideen, M., Wang, P., Pugh, D., Valera-Medina, A. (2023b). Evolution of ammonia reaction mechanisms and modelling parameters: A review. Applications in Energy and Combustion Science, 15, 100175. https://doi.org/10.1016/j.jaecs.2023.100175

[8] Kobayashi, H., Hayakawa, A., Somarathne, K. D. K. A., & Okafor, E. C. (2019). Science and technology of ammonia combustion. Proceedings of the Combustion Institute, 37(1),109–133. https://doi.org/10.1016/j.proci.2018.09.029

[9] Lee, J. H., Kim, J. H., Park, J. H., & Kwon, O. C. (2010). Studies on properties of laminar premixed hydrogen-added ammonia/air flames for hydrogen production. International Journal of Hydrogen Energy, 35(3),1054–1064. https://doi.org/10.1016/j.ijhydene.2009.11.071

[10] Li, J., Huang, H., Kobayashi, N., He, Z., & Nagai, Y.(2014). Study on using hydrogen and ammonia as fuels: Combustion characteristics and NO_x formation. International Journal of Energy Research, 38(9),1214–1223. https://doi.org/10.1002/er.3141

[11] Nozari, H., & Karabeyoğlu, A. (2015). Numerical study of combustion characteristics of ammonia as a renewable fuel and establishment of reduced reaction mechanisms. Fuel, 159, 223–233. https://doi.org/10.1016/j.fuel.2015.06.075

[12] Valera-Medina, A., Pugh, D. G., Marsh, P., Bulat, G., & Bowen, P. (2017). Preliminary study on lean premixed combustion of ammonia-hydrogen for swirling gas turbine combustors. International Journal of Hydrogen Energy, 42(38),24495–24503. https://doi.org/10.1016/j.ijhydene.2017.08.028

[13] Franco, M. C., Rocha, R. C., Costa, M., & Yehia, M.(2021). Characteristics of NH_3/H_2/Air Flames in a combustor fired by a swirl and bluff-body stabilized burner. Proceedings of the Combustion Institute, 38(4),5129–5138. https://doi.org/10.1016/j.proci.2020.06.141

[14] Xiao, H., Valera-Medina, A., & Bowen, P. J. (2017). Modeling combustion of ammonia/hydrogen fuel blends under gas turbine conditions. Energy & Fuels, 31(8),8631–8642. https://doi.org/10.1021/acs.energyfuels.7b00709

[15] Mathieu, O., & Petersen, E. L.(2015).Experimental and modeling study on the high-temperature oxidation of ammonia and related NO_x chemistry. Combustion and Flame, 162(3),554–570. https://doi.org/10.1016/j.combustflame.2014.08.022

[16] da Rocha, R. C., Costa, M., & Bai, X.-S. (2019). Chemical kinetic modelling of ammonia/hydrogen/air ignition, premixed flame propagation and NO emission. Fuel, 246, 24–33. https://doi.org/10.1016/j.fuel.2019.02.102

[17] Alnasif A., Mashruk S., Hayashi M., Jójka J., Shi H., Hayakawa A., &Valera-Medina A. (2023a). Performance investigation of currently available reaction mechanisms in the estimation of NO Measurements: A comparative study. Energies, 16(9),3847. https://doi.org/10.3390/en16093847

[18] Duynslaegher, C., Contino, F., Vandooren, J., Jeanmart, H. (2012). Modeling of ammonia combustion at low pressure. Combustion and Flame, 159, 2799–2805. https://doi.org/10.1016/j.combustflame.2012.06.003

[19] Nakamura, H., Hasegawa, S., Tezuka, T. Kinetic modeling of ammonia/air weak flames in a micro flow reactor with a controlled temperature profile. Combustion and Flame, 185, 16–27. https://doi.org/10.1016/j.combustflame.2017.06.021

[20] Alnasif A., Zitouni S., Mashruk S., Brequigny P., Kovaleva M., Mounaim-Rousselle C., &Valera-Medina A.(2023c).Experimental and numerical comparison of currently available reaction mechanisms for laminar flame speed in 70/30(%vol.) NH_3/H_2 flames. Applications in Energy and Combustion Science, 14, 100139. https://doi.org/10.1016/j. jaecs.2023.100139

[21] Stagni, A., Cavallotti, C., Arunthanayothin, S., Song, Y., Herbinet, O., Battin-Leclerc, F., Faravelli, T. (2020). An experimental, theoretical and kinetic-modeling study of the gas-phase oxidation of ammonia. Reaction Chemistry & Engineering, 5(4),696–711. https://doi.org/10.1039/C9RE00429G

[22] Munteanu, N., & Amzaini, S. M. (2018). Prediction of pollutant emissions from bluff-body stabilised non-premixed flames. Journal of Combustion, 2018, 1–11. https://doi.org/10.1155/2018/8924370

[23] Di Mauro, A., Ravetto, M., Goel, P., Baratta, M., Misul, D. A., Salvadori, S., Rothbauer, R., & Gretter, R. (2021). Modelling aspects in the simulation of the diffusive flame in a bluff-body geometry. Energies, 14(11),2992. https://doi.org/10.3390/en14112992

[24] Vigueras-Zúñiga, M. O., Tejeda-del-Cueto, M. E., Mashruk, S., Kovaleva, M., Ordóñez-Romero, C. L., & Valera-Medina, A. (2021). Methane/ammonia radical formation during high temperature reactions in swirl burners. Energies, 14(20),6624. https://doi.org/10.3390/en14206624

[25] Vigueras-Zúñiga, M. O., Tejeda-del-Cueto, M. E., Vasquez-Santacruz, J.-A., Herrera-May, A.-L., & Valera-Medina, A. (2020). Numerical predictions of a swirl combustor using complex chemistry fueled with ammonia/hydrogen blends. Energies, 13(2),288. https://doi.org/10.3390/en13020288

[26] Okafor, E. C., Naito, Y., Colson, S., Ichikawa, A., Kudo, T., Hayakawa, A., & Kobayashi, H.(2018).Experimental and numerical study of the laminar burning velocity of CH_4–NH_3–Air premixed flames. Combustion and Flame, 187, 185–198. https://doi.org/10.1016/j.combustflame.2017.09.002

[27] Valera-Medina, A., Gutesa, M., Xiao, H., Pugh, D., Giles, A., Goktepe, B., Marsh, R., & Bowen, P. (2019). Premixed ammonia/hydrogen swirl combustion under rich fuel conditions for gas turbines operation. International Journal of Hydrogen Energy, 44(16),8615–8626. https://doi.org/10.1016/j.ijhydene.2019.02.041

[28] Pugh, D., Bowen, P., Valera-Medina, A., Giles, A., Runyon, J., & Marsh, R.(2019).Influence of steam addition and elevated ambient conditions on NO_x reduction in a staged premixed swirling NH_3/H_2 flame. Proceedings of the Combustion Institute, 37(4),5401–5409. https://doi.org/10.1016/j.proci.2018.07.091

[29] Runyon, J., Marsh, R., Bowen, P., Pugh, D., Giles, A., & Morris, S. (2018). Lean methane flame stability in a premixed generic swirl burner: Isothermal flow and atmospheric combustion characterization. Experimental Thermal and Fluid Science, 92, 125–140. https://doi.org/10.1016/j.expthermflusci.2017.11.019

[30] Mikulčić, H., Baleta, J., Wang, X., Wang, J., Qi, F., & Wang, F. (2021). Numerical simulation of ammonia/methane/air combustion using reduced chemical kinetics models. International Journal of Hydrogen Energy, 46(45),23548–23563. https://doi.org/10.1016/j.ijhydene.2021.01.109

[31] Sudarma, A. F., Al-Witry, A., & Morsy, M. H. (2017). RANS numerical simulation of lean premixed bluff-body stabilized combustor: Comparison of turbulence models. Journal of Thermal Engineering, 3(3),1561–1573. https://doi.org/10.18186/journal-of-thermal-engineering.321093955

[32] Muppala, S. P. R., Manickam, B., & Dinkelacker, F. (2015). A comparative study of different reaction models for turbulent methane/hydrogen/air combustion. Journal of Thermal Engineering, 1(5),367–380. https://doi.org/10.18186/jte.76780

[33] Rajak, U., Nashine, P., Chaurasiya, P. K., & Verma, T. N. (2021). A numerical investigation of the species transport approach for modeling of gaseous combustion. Journal of Thermal Engineering, 7(Supplement 14),2054–2067. https://doi.org/10.18186/thermal.1051312

[34] Alnajideen, M., Shi, H., Northrop, W., Emberson, D., Kane, S., Czyżewski, P., Alnaeli, M., Mashruk, S., Rouwenhorst, K., Yu, C., Eckart, S., & Valera-Medina, A. (2024). Ammonia combustion and emissions in practical applications: A review. Carbon Neutrality, 3(1),13. https://doi.org/10.1007/s43979-024-00088-6

[35] Mashruk, S., Kovaleva, M., Alnasif, A., Chong, C. T., Hayakawa, A., Okafor, E. C., & Valera-Medina, A. (2022). Nitrogen oxide emissions analyses in ammonia/hydrogen/air premixed swirling flames. Energy, 260, 125183. https://doi.org/10.1016/j.energy.2022.125183

[36] Mashruk S., Kovaleva M., Chong C. T., Hayakawa A., Okafor E. C., &Valera-Medina A. (2021). Nitrogen oxides as a by-product of ammonia/hydrogen combustion regimes. Chemical Engineering Transactions, 89, 613–618. https://doi.org/10.3303/CET2189103

[37] Mashruk, S., Okafor, E. C., Kovaleva, M., Alnasif, A., Pugh, D., Hayakawa, A., & Valera-Medina, A.(2022).Evolution of N_2O production at Lean combustion condition in NH_3/H_2/air premixed swirling flames. Combustion and Flame, 244, 112299. https://doi.org/10.1016/j.combustflame.2022.112299

[38] Mashruk, S., Zhu, X., Roberts, W. L., Guiberti, T. F., & Valera-Medina, A. (2023). Chemiluminescent footprint of premixed ammonia-methane-air swirling flames. Proceedings of the Combustion Institute, 39(1),1415–1423. https://doi.org/10.1016/j.proci.2022.08.073

[39] Valera-Medina, A., Marsh, R., Runyon, J., Pugh, D., Beasley, P., Hughes, T., & Bowen, P. (2017). Ammonia–methane combustion in tangential swirl burners for gas turbine power generation. Applied Energy, 185, 1362–1371. https://doi.org/10.1016/j.apenergy.2016.02.073

[40] Shaddix, C.R.(2017).A new method to compute the proper radiant heat transfer correction of bare-wire thermocouple measurements. Paper presented at the 10th U.S. National Combustion Meeting, College Park, MD.

[41] British Standards Institution. (1996). Gas turbines – Exhaust gas emission(BS ISO 11042-1:1996). London: Author.

[42] Richards, K.J., Senecal, P.K., & Pomraning, E. (2024), CONVERGE 3.0 [Computer Software], Madison, WI: Convergent Science.

[43] Gulsan, M. A., & Boke, Y. E. (2024). CFD validation of unconfined low swirl burner under cold flow conditions. In *Proceedings of INCOS 2024: International Combustion Symposium* (pp. 65–77). Bursa, Turkey: Uludağ University.

[44] Valera-Medina, A., Mashruk, S., Xiao, H., Chiong, M.-C., & Chong, C. T.(2020).Ammonia/hydrogen blends for zero-carbon energy. Paper presented at the 8th International Conference on Fluid Mechanics(Virtual, 25-28 September 2018).

[45] Baej, H., Valera Medina, A., Syred, N., Marsh, R., &Bowen, P.J.(2015).CFD predictions of swirl burner aerodynamics with variable outlet configurations. In Proceedings of the Global Conference on Energy and Sustainable Development (GCESD 2015) (pp. 2307–2312).Coventry, UK.

[46] Eriksson P. (2007). The Zimont TFC model applied to premixed bluff-body stabilized combustion using four different RANS turbulence models. In Proceedings of the ASME Turbo Expo 2007 (Paper No. GT2007-27480). https://doi.org/10.1115/GT2007-27480